GEOPHYSICAL RESEARCH LETTERS, VOL. 23, NO. 14, PAGES 1829-1832, JULY 1, 1996

Genetic algorithm inversion for receiver functions with application to crust and uppermost mantle structure beneath Eastern Australia

Takuo Shibutani

Disaster Prevention Research Institute, Kyoto University, Uji, Japan

Malcolm Sambridge and Brian Kennett

Research School of Earth Sciences, Australian National University, Canberra, Australia

Abstract. Genetic algorithm (GA) inversion, a nonlinear global optimization technique, has been applied to determine crustal and uppermost mantle velocity structure from teleseismic receiver functions. With a new modelling in which not only the S wave velocity but also the layer thickness and the V_P/V_S ratio are model parameters, the GA receiver function inversion is able to recover the velocity structure with reasonable accuracy in the whole crust, and particularly well for the surface layer and the crust-mantle boundary. Structural inversion for receiver functions from a network of broadband seismic stations in eastern Australia allows a comparison of crustal structure from different tectonic environments. The crust-mantle boundary is shallow and sharp on the craton but deep and transitional along the axis of the fold belt zone in eastern Australia. This suggests crustal thickening in the fold belt by underplating or intrusion of mantle materials into the lower crust.

Introduction

The coda of teleseismic P waves contains a significant amount of information on seismic structure in the vicinity of the receiver. The influence of the source can be largely eliminated by source equalization in which the radial component of motion is deconvolved with the vertical component to generate a receiver function [*Langston*,1979] which isolates conversions from P to S generated at boundaries beneath the recording site. The receiver function waveform can be inverted in the time domain for a 1-D shear wave velocity model of the crust and uppermost mantle beneath the receiver [*Owens et al.*, 1984; *Kosarev et al.*, 1993; *Kind et al.*, 1995].

The receiver function depends nonlinearly on the shear wavespeed in both amplitude and time. In previous studies, a linearization procedure has been used to invert the receiver function which requires the initial model to be close to the true velocity structure, which is difficult to ensure. The results of the synthetic tests by *Ammon et al.* [1990] clearly showed that the final models were dependent on the initial models.

In order to overcome the problems with the previous methods, we employ a genetic algorithm (GA) [*Holland*, 1975; *Goldberg*, 1989] to invert the receiver function. We develop a novel procedure to exploit the information from the best fitting trials by making an 'average' model which is more stable and less dependent on the starting assumptions. Because a wide range of possible solutions can be sampled, the extent of the errors and nonuniqueness can be assessed in the solutions.

Implementation of the method and synthetic testing

A Gaussian high-cut filter was applied to each receiver function to eliminate frequencies above 1 Hz and so minimize influence from small scale heterogeneities. The receiver functions from $6-18$ teleseismic events at each station were stacked for a set of ranges of backazimuths. The stacking weights emphasize receiver functions with higher signal-to-noise ratios and those whose backazimuth and incident angle were closer to the mean for the set of events. The radial component of the stacked receiver function was then inverted for a 1-D velocity model beneath each station.

In our inversion, we have modeled the crust and uppermost mantle down to 60 km with six major layers: a sediment layer, basement layer, upper crust, middle crust, lower crust and uppermost mantle. The model parameters in each layer are the thickness, the S wave velocity at the upper boundary, the S wave velocity at the lower boundary and the velocity ratio between P and S waves (V_P/V_S). The S wave velocity in each layer is constructed by linearly connecting the values at the upper and lower boundaries, to give a sequence of constant velocity gradient segments separated by velocity discontinuities.

Genetic algorithms are finding an increasing number of applications in geophysical problems [*Stoffa and Sen*,

Paper number 96GL01671
0094-8534/96/96GL-01671$05.00

1991; *Zhou et al.* 1995]. The algorithm used here is described in detail in *Sambridge and Drijkoningen* [1992]. The only variant is that we use a rank-based selection scheme (tournament selection) as opposed to a direct 'misfit'-based scheme [*Sambridge and Gallagher*, 1993]. For each model parameter, upper and lower bounds and 2^n possible values are specified. The ranges of the model parameters, the n values and incremental values are shown in Table 1. The size of the model space to be searched is $2^{85} \approx 3.87 \times 10^{25}$. Beginning with a randomly generated initial population of 50 models and corresponding misfit values which are defined by square sum of the difference between the receiver function predicted for each model and that obtained from observed waveforms, succeeding populations are created by selection, crossover and mutation. The action of these three operations is controlled by random processes with threshold probability 0.75 for selection, 0.85 for crossover and 0.009 for mutation; these parameters were chosen after a sequence of trials. This procedure was iterated for 200 generations; as a result 10,000 models were generated, checked during each inversion and used in the generation of a stable 'average' model.

The GA is particularly well suited to implementation on a parallel computer because each calculation of the forward problem may be performed on a different processor. We used a parallel computer (CM-5) with a message-passing-interface protocol (p4) to perform the inversions. This reduced the computation time to about one tenth of that with a workstation (SPARCstation10).

A stacked radial component of synthetic receiver functions with added noise to an assumed 'true' model has been inverted with the GA method. The results of several inversions indicate that differences in the S wave velocity between the resulting models and the 'true' model are very small ($\leq$ 4 %) in the shallower parts ($\leq$ 3 km) and at greater depths ($\geq$ 20 km). At middle depths (3–20 km) the deviations are a little larger, however, they are at most 10 %. The V_P/V_S ratio is well recovered in the upper part of the model ($\leq$ 25 km), especially in the sediment layer, but the performance is less good at depth.

Application to observed data

The GA receiver function inversion method has been applied to broadband waveforms from the SKIPPY project in eastern Australia [*van der Hilst et al.*, 1993] to find the crustal and uppermost mantle seismic velocity structure beneath each of the stations. The SKIPPY project is designed to cover the Australian continent with broadband stations at a spacing of around 400 km, and so provides an opportunity for systematic study of crustal structure.

The results for SB01, SB02, SA07 and SA08 are shown in Fig.1 (see also Fig.3 for the location of the stations). Solid lines indicate averaged models for the S wave velocity and the V_P/V_S ratio which are generated by weighting the best 1,000 models by the inverse of their misfit values. For the S wave velocity, regions sampled by the best 1,000 models are shown darker gray shaded areas. Waveform matches between receiver functions obtained from observed waveforms and calculated on the best 1,000 models are shown in Fig.2. Since the fit for major phases is good and the deviations of the

Table 1. Model parameters in the GA receiver function inversion

		Sediment	Basement	Crust			Mantle
				upper	middle	lower	
Thickness (km)	*lower*	0.0	0.0	5.0	5.0	0.0	5.0
	upper	2.0	3.0	20.0	20.0	15.0	20.0
	n	3	3	4	4	4	4
	increment	0.286	0.429	1.000	1.000	1.000	1.000
V_S(upper) (km/s)	*lower*	0.50	1.30	2.90	3.40	3.70	4.00
	upper	1.50	3.30	3.90	4.40	4.70	5.00
	n	4	5	4	4	4	4
	increment	0.067	0.064	0.067	0.067	0.067	0.067
V_S(lower) (km/s)	*lower*	0.50	1.30	2.90	3.40	3.70	4.00
	upper	1.50	3.30	3.90	4.40	4.70	5.00
	n	4	5	4	4	4	4
	increment	0.067	0.064	0.067	0.067	0.067	0.067
V_P/V_S	*lower*	2.00	1.65	1.65	1.65	1.65	1.70
	upper	3.00	2.00	1.80	1.80	1.80	1.90
	n	3	2	2	2	2	2
	increment	0.143	0.117	0.050	0.050	0.050	0.067
Q_α		100	675	1450	1450	1450	1450
Q_β		25	300	600	600	600	600

V_S(upper) and V_S(lower) are the S wave velocity at the upper and the lower boundaries in each layer. *lower* and *upper* for the four variables indicate the lower and the upper bounds in which the variables can have 2^n values. Q_α and Q_β are fixed in each layer.

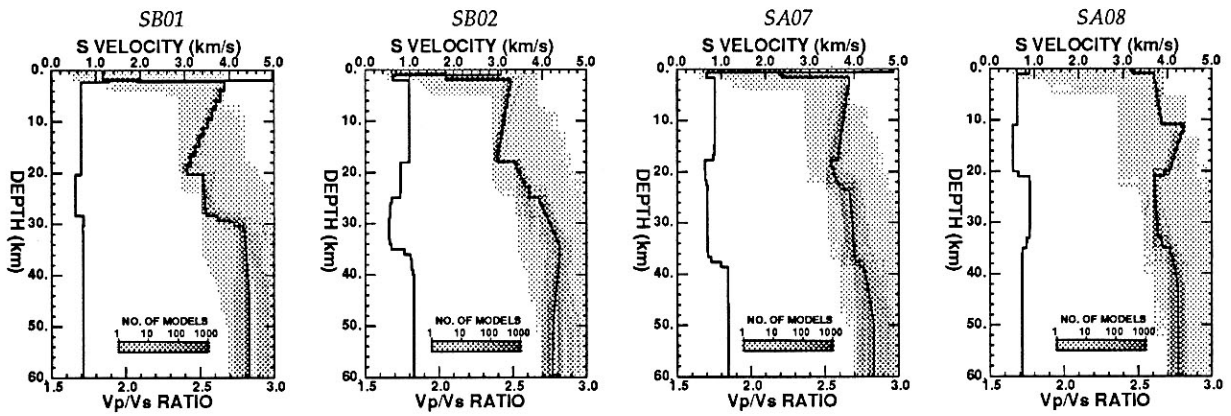

Figure 1. Seismic velocity models for SB01, SB02, SA07 and SA08. For the S wave velocity, all 10,000 models searched in the GA inversion are shown as the light gray shaded area. The best 1,000 models are shown as the darker gray shaded area. The darkness is logarithmically proportional to the number of the models as shown by the gray scale bar. The averaged model (see the text for details) are shown by the black solid line. For the V_P/V_S, the solid line indicates the averaged model.

predicted receiver functions almost lie within those of the receiver functions obtained from the observed data, the best 1,000 models can be thought of as acceptable models. We can assess the errors in the solutions by the extent of the darker gray areas in Fig.1.

The S wave velocity profiles for SB01, SB02 and SA07 have a sediment layer with a very slow velocity (0.7 – 1.2 km/s) and a very high V_P/V_S ratio (2.4 – 2.9) at their top, while the top layer of SA08 is a basement layer with $V_S = 3.2$ and $V_P/V_S = 1.8$. These features are consistent with the surface geology since SB01, SB02 and SA07 are located on sedimentary basins whereas SA08 is located on an orogenic province. The sediment layer makes the waveform complicated as illustrated for SB01, SB02 and SA07 in Fig.2. Note that P-to-S converted phases and reverberations (1 – 3 s) originating in the sediment layer are larger than the direct P phase which is expected at 0 s. The predicted receiver functions explain well the complicated features in the receiver functions obtained from the observed data.

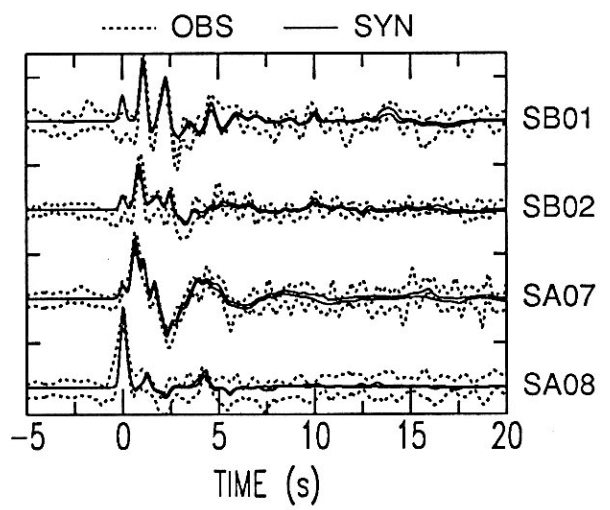

Figure 2. Waveform matches between the receiver functions (dotted lines) obtained from observed waveforms and the predicted receiver functions (solid lines) based on the best 1,000 models. Both lines show ±1 standard deviation bounds.

Synthetic tests indicate that the character of the crust-mantle boundary can be well determined. The depth of the boundary was estimated at each station; for a transitional zone between crust and mantle the lower boundary was selected, for examples, 30 km for SB01, 35 km for SB02, 38 km for SA07 and 36 km for SA08. The P-to-S converted phase generated at the crust-mantle boundary is expected to be observed at 4 – 5 s after the direct P phase if the boundary is located at 30 – 40 km. In Fig.2 a very clear phase corresponding to the P-to-S converted phase can be seen at 4.6 s for SB01 and a quite clear phase at 4.2 s for SA08, however, no clear phase for SB02 and SA07. Consequently the resulting model has a sharp boundary for SB01 and a intermediate one for SA08, whereas those for SB02 and SA07 have a broad transitional boundary.

Fig.3 displays the depth and nature of the boundary superimposed on a contour map combining the present results with those from previous refraction surveys compiled by *Collins* [1991] indicated by crosses. This study has significantly improved the available data coverage. The eastern part of the Australian continent has been built by the fusion of the Paleozoic 'Tasman Fold Belt' on to the Precambrian craton region to the west [*Doutch and Nicholas*, 1978]. The crust-mantle boundary is deep (38 – 44 km) and mostly transitional in character along the axis of the fold belt zone in the east (from stations: ZB12, SB09 to SA05, SA03). This feature agrees well with negative anomalies in the Bouguer gravity, which can be interpreted as the region where the crust is thick (since the crustal materials are lighter than the mantle materials). A relatively sharp Moho is found at a shal-

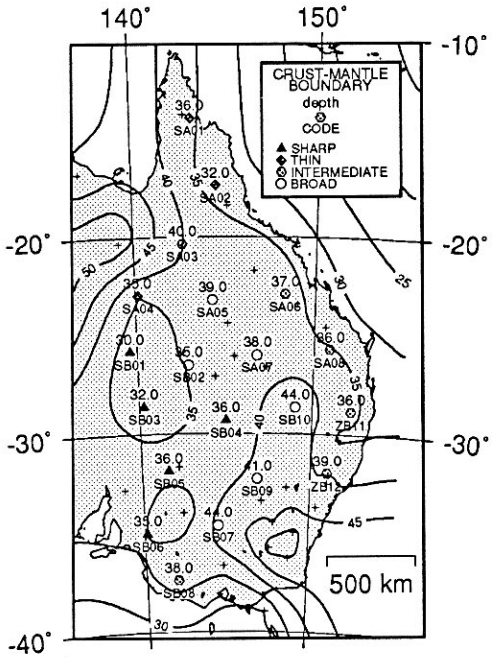

Figure 3. The depth of the crust-mantle boundary beneath eastern Australia. The type of the crust-mantle boundary is classified into four categories : 'SHARP' ($\leq$ 2 km), 'THIN' ($\leq$ 5 km), 'INTERMEDIATE' ($\leq$ 10 km), and 'BROAD' ($>$ 10 km). The crosses indicate the points beneath which the crustal structure was obtained by previous refraction surveys [Collins, 1991]. The data were used to draw the contours in combination with our inversion results.

lower depth (30 – 36 km) at the western edge of the study area close to the boundary between Phanerozoic and Precambrian exposure [*Hill*, 1951]. These features of the crust-mantle boundary suggest that the crust in the fold belt zone has been thickened along its axis perhaps by underplating or intrusion of mantle materials into the lower crust. This crustal thickening might have occurred when the Australian continent broke up from a supercontinent at about 600 Ma and consequently young plates followed by ridges subducted beneath the Australian continent from east to west, which supplied a large amount of mantle materials into the lower crust.

The SKIPPY stations now extend across the central and western craton region, and it will be very interesting to compare the results for the craton region with that for the eastern fold belt zone studied here and to examine the questions of the differences in crustal structure and their cause.

Acknowledgments. T. Shibutani was supported by a research scholarship from the Japanese Ministry of Education and would like to thank the Research School of Earth Sciences for hospitality and access to the SKIPPY data. We would like to thank R. van der Hilst for his useful advice on the data and O. Gudmundsson and K. Creager for their advice on the method. The calculations were performed in part on the parallel computer CM-5 at the Centre for Information Science Research, Australian National University.

References

Ammon, C.J., G.E. Randall, and G. Zandt, On the nonuniqueness of receiver function inversions, *J. Geophys. Res., 95*, 15,303–15,318, 1990.

Collins, C.D.N., The nature of the crust-mantle boundary under Australia from seismic evidence, *Geol. Soc. Aust. Spec. Publ.,17*, 67–80, 1991.

Doutch, H.F., and E. Nicholas, The Phanerozoic sedimentary basins of Australia and their tectonic implications, *Tectonophysics, 48*, 365–388, 1978.

Goldberg, D.E., *Genetic Algorithms in Search, Optimization,and Machine Learning*, Addison-Wesley, Reading, MA, 1989.

Hill, D., Geology. In: Handbook of Queensland, Aust. N.Z. Assoc. Adv. Sci., Brisbane, 13–24, 1951.

Holland, J.H., *Adaptation in Natural and Artificial Systems*, University of Michigan Press, Ann Arbor, 1975.

Kind, R., G.L. Kosarev, and N.V. Petersen, Receiver functions at the stations of the German Regional Seismic Network (GRSN), *Geophys. J. Int., 121*, 191–202, 1995.

Kosarev, G.L., N.V. Petersen, L.P. Vinnik, and S.W. Roecker, Receiver functions for the Tien Shan analog broadband network: Contrasts in the evolution of structures across the Talasso-Fergana fault, *J. Geophys. Res., 98*, 4437–4448, 1993.

Langston, C.A., Structure under Mount Rainier, Washington,inferred from teleseismic body waves, *J. Geophys. Res., 84*, 4749–4762, 1979.

Owens, T.J., G. Zandt and S.R. Taylor, Seismic evidence for an ancient rift beneath the Cumberland Plateau, Tennessee: A detailed analysis of broadband teleseismic *P* waveforms, *J. Geophys. Res., 89*, 7783–7795, 1984.

Sambridge, M., and G. Drijkoningen, Genetic algorithms in seismic waveform inversion, *Geophys. J. Int., 109*, 323–342, 1992.

Sambridge, M., and K. Gallagher, Earthquake hypocenter location using genetic algorithms, *Bull. Seism. Soc. Am., 83*, 1467–1491, 1993.

Stoffa, P.L., and M.K. Sen, Nonlinear multiparameter optimization using genetic algorithms: Inversion of plane-wave seismograms, *Geophysics, 56*, 1794–1810, 1991.

van der Hilst, R., B. Kennett, D. Christie, and J. Grant, Project Skippy explores the lithosphere and Mantle beneath Australia, *EOS, 75*, 177–181, 1994.

Zhou, R., F. Tajima, and P. L. Stoffa, Earthquake source parameter determination using genetic algorithms, *Geophys. Res. Lett., 22*, 517–520, 1995.

T. Shibutani, Disaster Prevention Research Institute, Kyoto University, Uji, Kyoto 611, Japan. (e-mail: shibutan@rcep.dpri.kyoto-u.ac.jp)

M. Sambridge and B. Kennett, Research School of Earth Sciences, Australian National University, Canberra, ACT 0200, Australia. (e-mail: malcolm@rses.anu.edu.au, brian@rses.anu.edu.au)

(received December 22, 1995;
revised May 13, 1996; accepted May 14, 1996.)